Supporting Information *for*

A universal fluorometric assay strategy for glycosidases based on functional carbon quantum dots: β-galactosidase activity detection in vitro and in living cells

Cong Tang,[a†] *Jin Zhou,*[b†] *Zhaosheng Qian,*[a†] *Yanyan Ma,*[a] *Yuanyuan Huang,*[a] *and Hui Feng*[a]*

[a] College of Chemistry and Life Science, Zhejiang Normal University, Jinhua 321004, P. R. China

[b] College of Pharmacy, Weifang Medical University, Weifang 261053, P. R. China

β-CD-CQDs in the presence of varying amount of *p*-NP. (B) The relationship between τ_0/τ and the concentration of *p*-NP. The lifetime of β-CD-CQDs is not changed as the addition of *p*-NP.

8. Figure S8 Comparison between the UV-visible spectrum of *p*-NP and the fluorescence emission spectrum of β-CD-CQDs nanoprobe.

9. Figure S9 The fluorescence intensity of β-CD-CQDs nanoprobe as a function of incubation time in the presence of NPGal (200.0 μM) and varying level of β-Gal (50.0, 100.0. 150.0 and 200.0 U/L).

10. Figure S10 (A) Fluorescence spectra of the mixture containing β-CD-CQDs nanoprobe and NPGal (150.0 μM) as increasing level of β-Gal from 0.0 to 100.0 U/L. (B) The fluorescence intensity of the nanoprobe versus β-Gal activity. Inset: the fitting curve between fluorescence intensity and β-Gal level.

11. Figure S11 (A) Fluorescence spectra of the mixture containing β-CD-CQDs nanoprobe and NPGal (300.0 μM) as increasing level of β-Gal from 0.0 to 100.0 U/L. (B) The fluorescence intensity of the nanoprobe versus β-Gal activity. Inset: the fitting curve between fluorescence intensity and β-Gal level.

12. Figure S12 (A) Fluorescence spectra of the mixture containing β-CD-CQDs nanoprobe, NPGal (200.0 μM) and β-Gal (100.0 U/L) in the presence of different concentrations of D-galactal (from bottom to top): 0.0, 50.0, 100.0, 200.0, 300.0, 400.0, 500.0 and 600.0 μM, respectively. (B) The fitting curve between inhibition efficiency and concentration of D-galactal.

13. Figure S13 Effect of β-CD-CQDs with various concentrations (10.0 – 200.0 μg/mL) on the OVCAR3 cells.

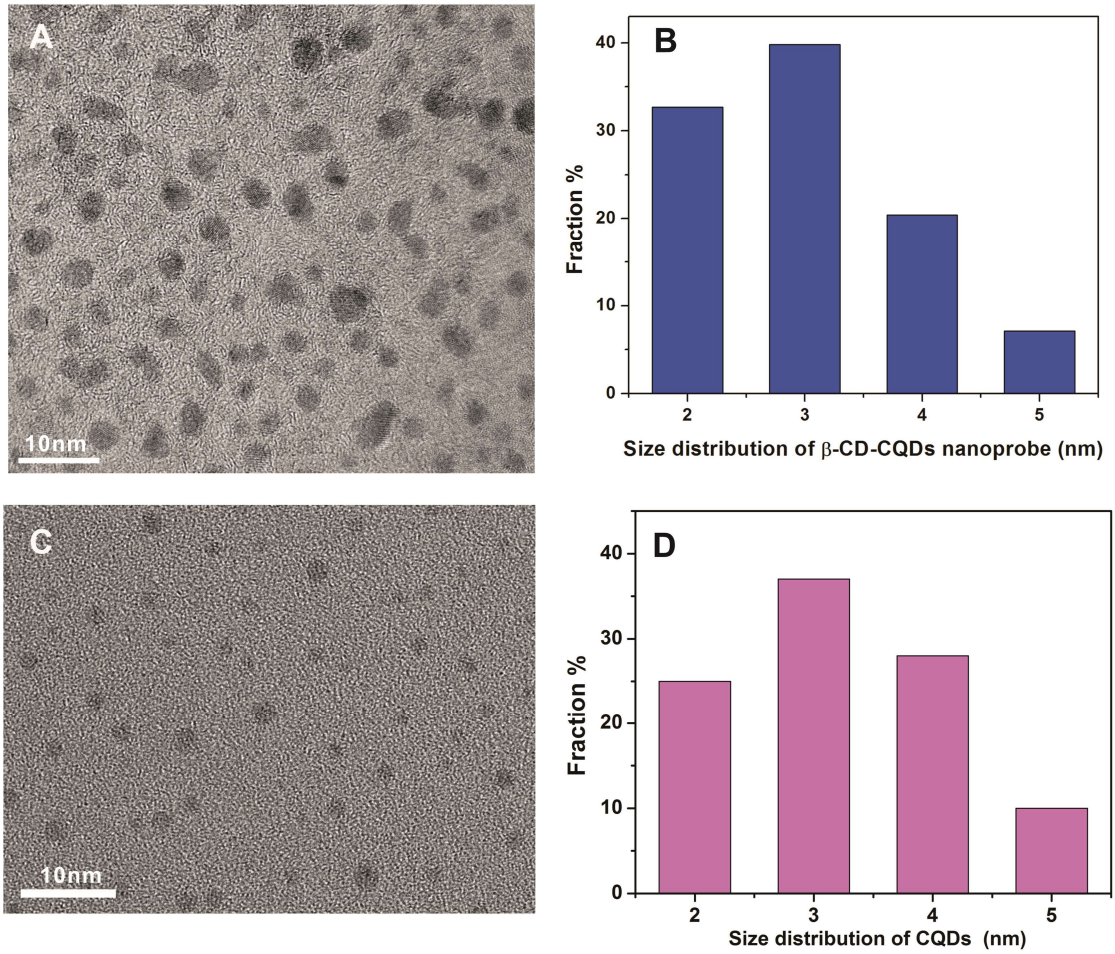

Figure S1. TEM image (A) and size distribution in diameter (B) of β-CD-CQDs nanoprobe, and TEM image (C) and size distribution in diameter (D) of pure CQDs.

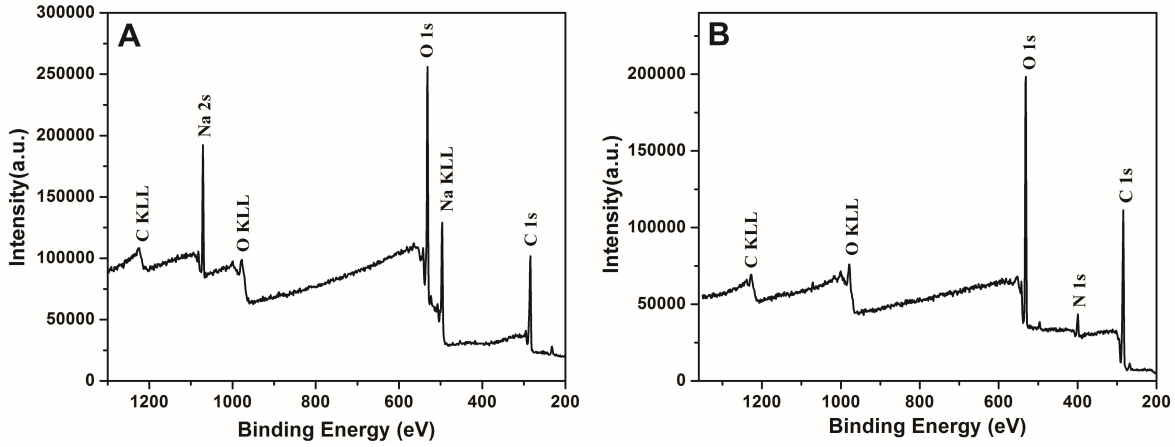

Figure S2. XPS wide spectra of pure CQDs (A) and β-CD-CQDs nanoprobe (B).

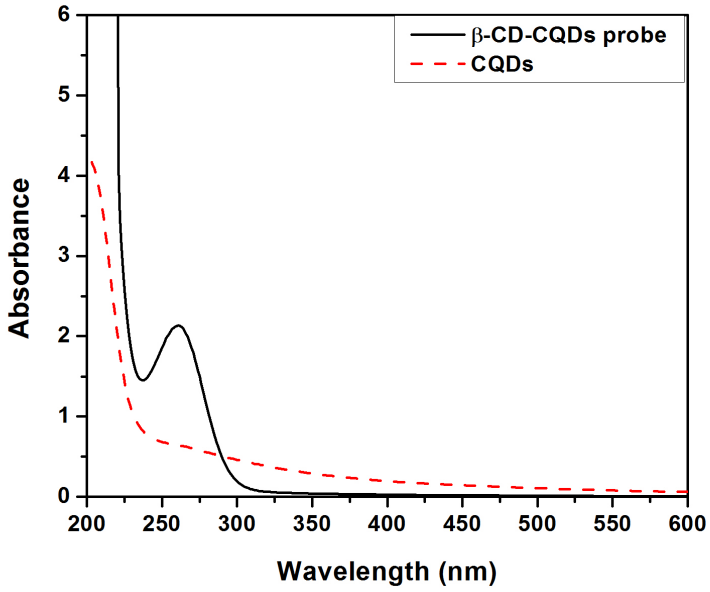

Figure S3. UV-visible spectra of CQDs and β-CD-CQDs nanoprobe.

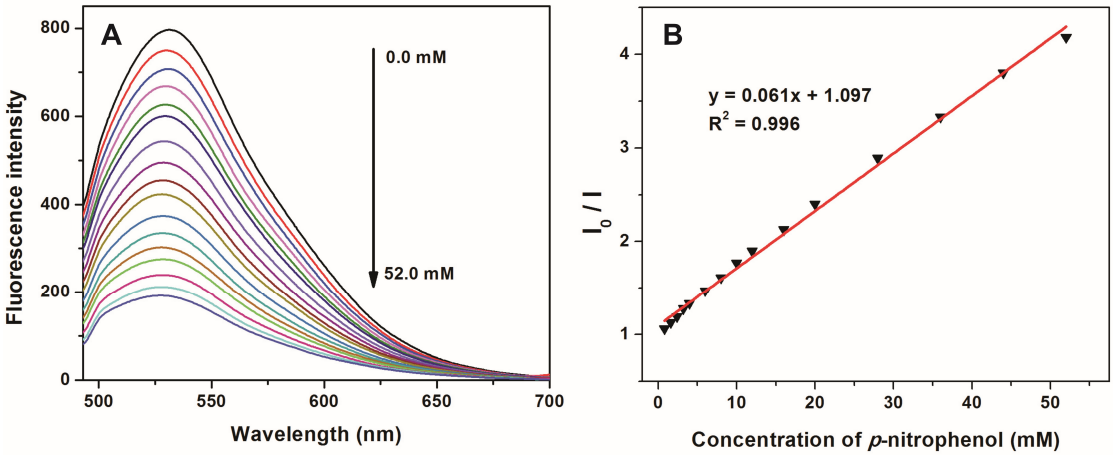

Figure S4. (A) The fluorescence spectra of CQDs as a function of *p*-NP concentration in the range of 0.0 – 52.0 mM. (B) Linear fitting curve between quenching efficiency I_0/I and the concentration of *p*-NP according to Stern-Volmer equation.

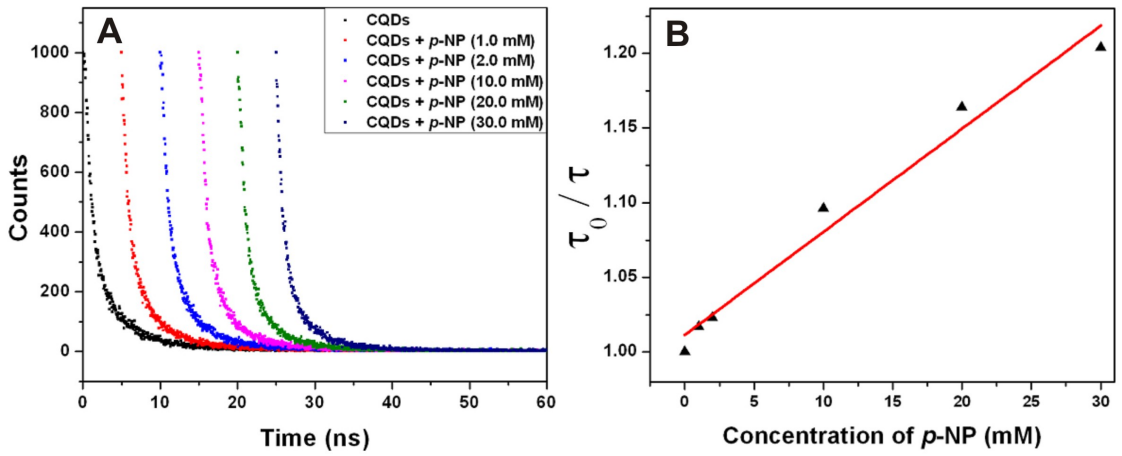

Figure S5. (A) Comparison of time-resolved fluorescence decay curves of CQDs in the presence of varying amount of *p*-NP. (B) Linear fitting curve between τ_0/τ and the concentration of *p*-NP according to Stern-Volmer equation. The lifetime of CQDs decreases as the addition of *p*-NP.

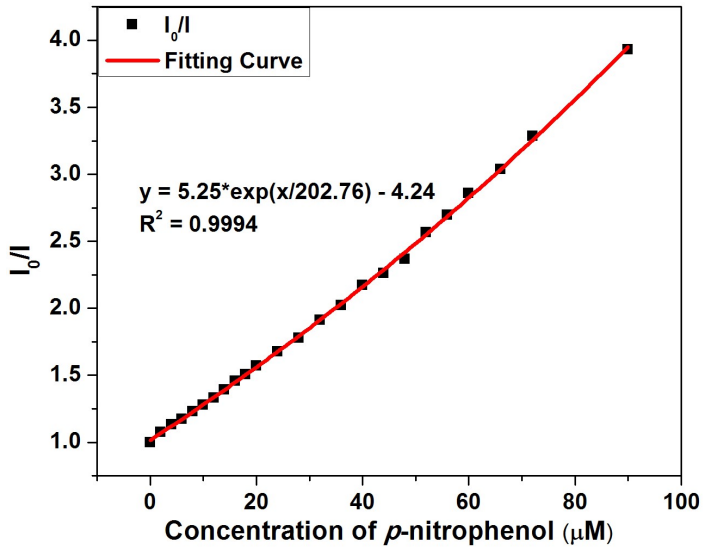

Figure S6 Linear fitting curve between quenching efficiency I_0/I for β-CD-CQDs and the concentration of *p*-NP according to Perrin's model.

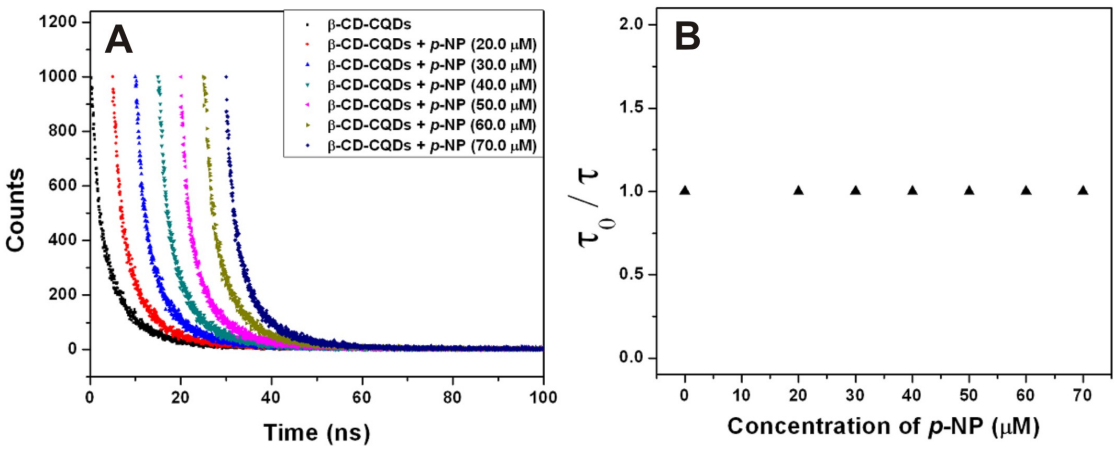

Figure S7. (A) Comparison of time-resolved fluorescence decay curves of β-CD-CQDs in the presence of varying amount of *p*-NP. (B) The relationship between τ_0/τ and the concentration of *p*-NP. The lifetime of β-CD-CQDs is not changed as the addition of *p*-NP.

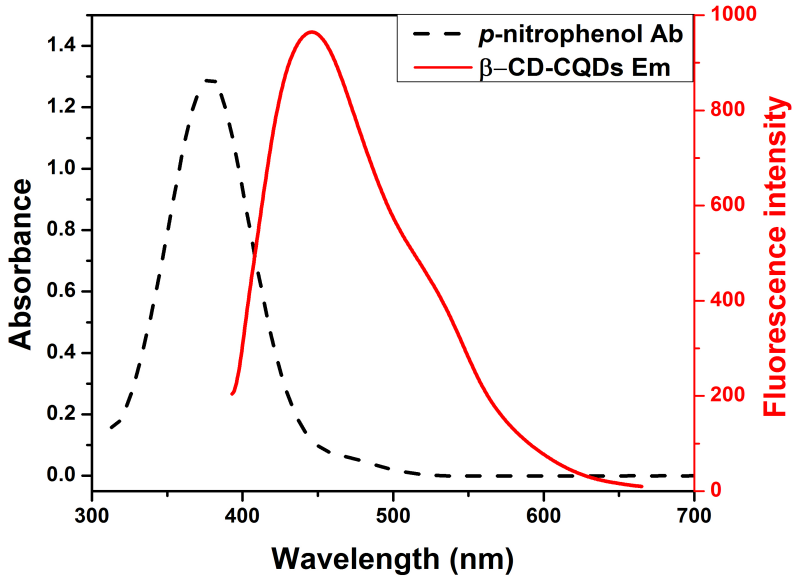

Figure S8 Comparison between the UV-visible spectrum of *p*-NP and the fluorescence emission spectrum of β-CD-CQDs nanoprobe in PBS solution (pH 7.4).

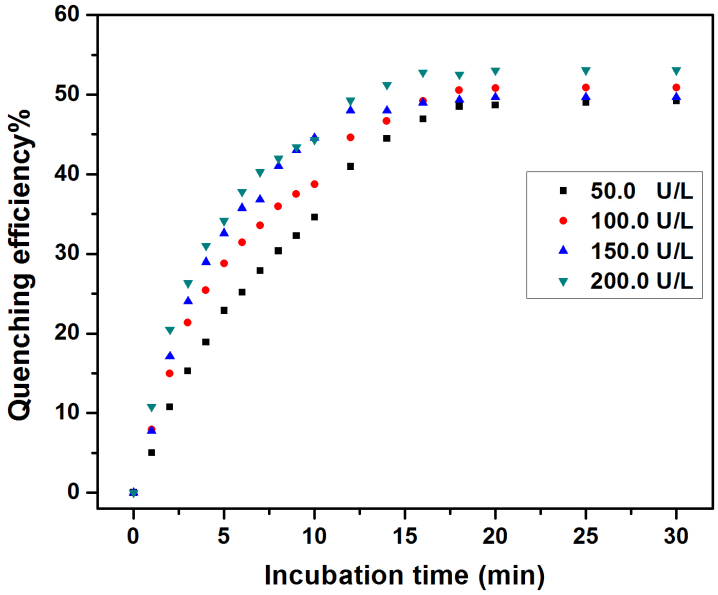

Figure S9 The fluorescence intensity of β-CD-CQDs nanoprobe as a function of incubation time in the presence of NPGal (200.0 μM) and varying level of β-Gal (50.0, 100.0. 150.0 and 200.0 U/L).

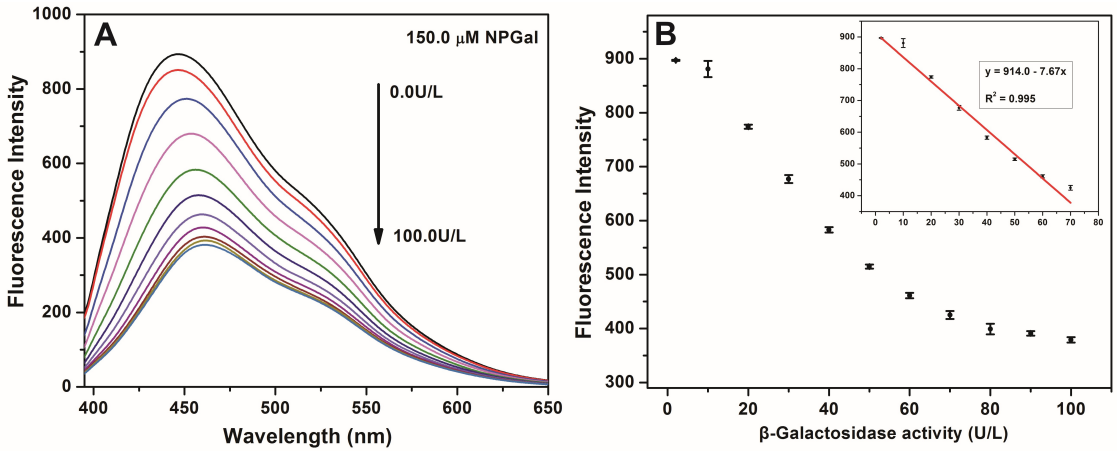

Figure S10 (A) Fluorescence spectra of the mixture containing β-CD-CQDs nanoprobe and NPGal (150.0 μM) as increasing level of β-Gal from 0.0 to 100.0 U/L. (B) The fluorescence intensity of the nanoprobe versus β-Gal activity. Inset: the fitting curve between fluorescence intensity and β-Gal level. The detection limit was calculated as 0.6 U/L, and the linear range is 2.0 – 70.0 U/L.

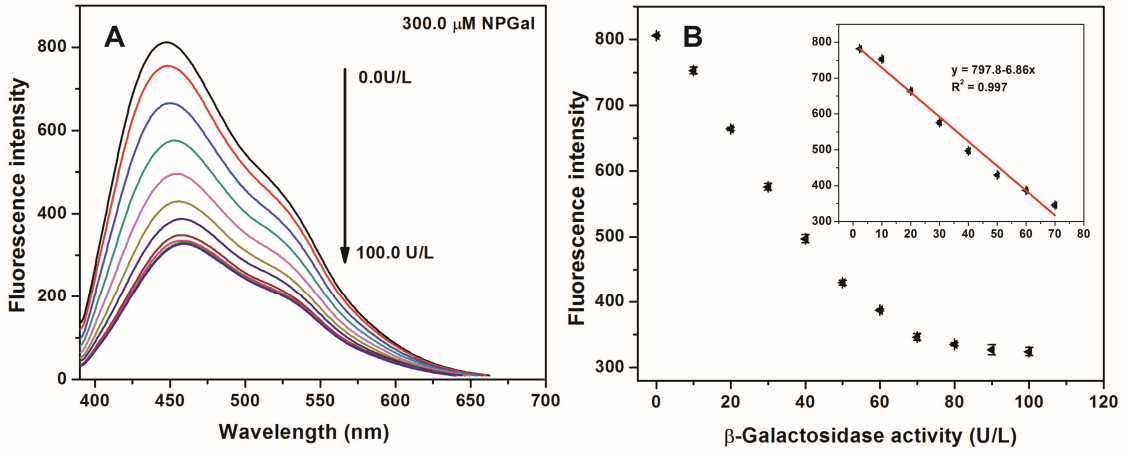

Figure S11 (A) Fluorescence spectra of the mixture containing β-CD-CQDs nanoprobe and NPGal (300.0 μM) as increasing level of β-Gal from 0.0 to 100.0 U/L. (B) The fluorescence intensity of the nanoprobe versus β-Gal activity. Inset: the fitting curve between fluorescence intensity and β-Gal level. The detection limit was calculated as 0.7 U/L, and the linear range is 2.3 – 70.0 U/L.

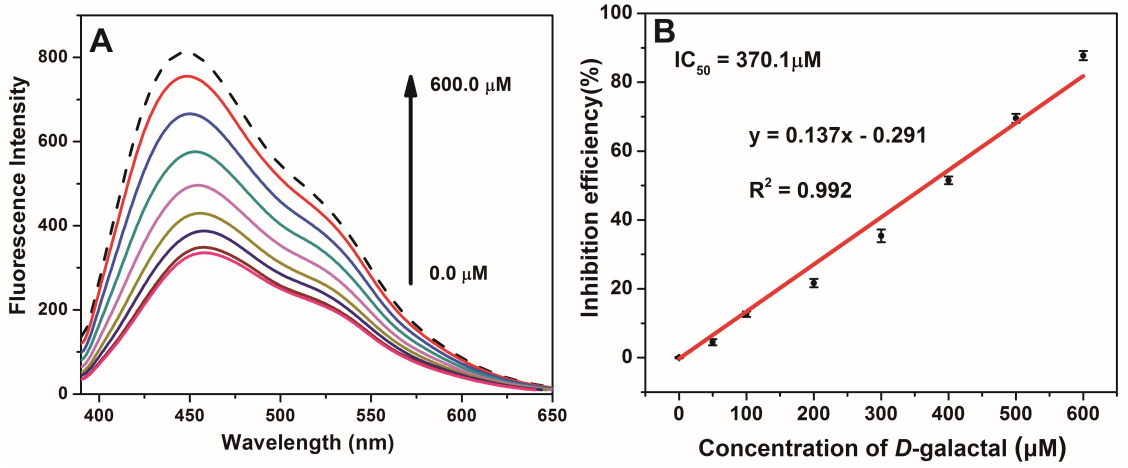

Figure S12 (A) Fluorescence spectra of the mixture containing β-CD-CQDs nanoprobe, NPGal (200.0 μM) and β-Gal (100.0 U/L) in the presence of different concentrations of D-galactal (from bottom to top): 0.0, 50.0, 100.0, 200.0, 300.0, 400.0, 500.0 and 600.0 μM, respectively. (B) The fitting curve between inhibition efficiency and concentration of D-galactal.

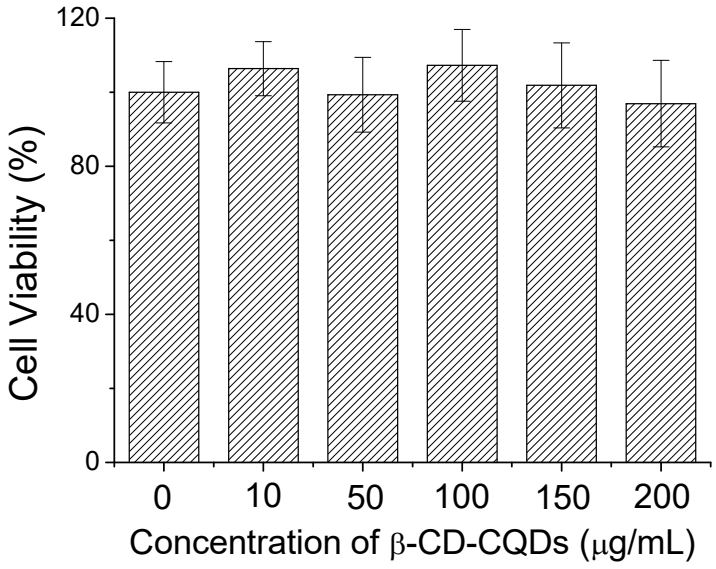

Figure S13 Effect of β-CD-CQDs with various concentrations (10.0 – 200.0 μg/mL) on the OVCAR3 cells. The viability of cells without is defined as 100%. The results are the mean ± standard deviation of five separate measurements.